

Investigation on Anti/De-icing Performance of an Innovative Electrothermal Structure

GU Jianzhen¹, QI Huimin^{1*}, YU Jiabin¹, ZHANG Yafeng¹, GU Xingshi²

1. Key Laboratory of Testing Technology for Manufacturing Process, Ministry of Education, Southwest University of Science and Technology, Mianyang 621010, P.R.China;

2. Key Laboratory of Icing and Anti/De-icing, China Aerodynamics Research and Development Center, Mianyang 621000, P.R.China

(Received 20 March 2023; revised 30 August 2023; accepted 1 September 2023)

Abstract: Innovative development of an anti- and de-icing system which can be practically used for aircraft wings is an ongoing challenge. High energy-consumption of electrothermal anti-icing/de-icing in aircraft is a tough problem up to date. In this work, we design an anti/de-icing structure based on the electric heating. The electrothermal structure is composed of the polydimethylsiloxane (PDMS) insulation coating, conductive layer, electrothermal layer and porous insulation layer from the top to the bottom. The effect of the thickness of the conductive silver paste layer and the content of the conductive liquid on the temperature of the insulation layer and the insulation layer under different power levels is investigated. The results indicate that at room temperature, when the input power is 4 W and the thickness of the silver slurry layer is 300 μm , the maximum temperature of the insulation layer can reach 134 $^{\circ}\text{C}$. Moreover, when the input power is 18 W, the top temperature can quickly reach 0 $^{\circ}\text{C}$, while the bottom temperature remains around -12.5°C at -20°C , resulting in less energy loss. Our study can provide theoretical guidance for the design of electric heating anti-icing material systems.

Key words: anti/de-icing; electrothermal structure; polydimethylsiloxane; heat transfer; energy utilization

CLC number: V19 **Document code:** A **Article ID:** 1005-1120(2023)S1-0096-09

0 Introduction

The ice accretion on transportation, aircraft surfaces, etc., is a critical issue^[1-2]. The disastrous problems induced by icing, such as collapse of energy transmission systems and aircraft crashes, can cause heavy losses of property and human casualties. Therefore, it is urgent to explore an excellent method for de-icing to ensure the safety of normal life. Generally, the mechanical de-icing is used in power lines. The disadvantages of the approach is the high labor intensity and the low de-icing efficiency. The common approaches used in aircraft to remove accreted ice are dominated by electrothermal and aerothermal technologies^[2-4], but the above methods will lead to the high energy consumption

which further enhances the cost.

In particular, the anti/de-icing methods can be divided into three categories, including passive, active and active-passive composite methods according to the energy input mode^[5-7]. The passive anti/de-icing method does not require the energy input. The icing surface is superhydrophobic, and the icing adhesion strength is very low. The ice can fall off naturally under the external aerodynamic force, making the surface unable to accumulate ice. Passive anti/de-icing methods mainly include the super-slip surface, the micro-nano super-hydrophobic surface, and the low surface energy surface, etc.^[8-10] Moreover, the passive anti/de-icing methods display good results in laboratory, but can be hardly used under the practical conditions, considering the

*Corresponding author, E-mail address: huimqi@swust.edu.cn.

How to cite this article: GU Jianzhen, QI Huimin, YU Jiabin, et al. Investigation on anti/de-icing performance of an innovative electrothermal structure[J]. Transactions of Nanjing University of Aeronautics and Astronautics, 2023, 40(S1):96-104.

<http://dx.doi.org/10.16356/j.1005-1120.2023.S1.009>

service life and cost^[11-12]. Generally, the active anti/de-icing method is to make the ice fall off through the external input energy, mainly including electric heating anti/de-icing, gas heating anti-icing and vibration anti-icing^[13-14]. The active anti/de-icing method is relatively mature and has been successfully used in aircraft, wind turbine blades and other fields^[15-17], but the current anti/de-icing method consumes a lot of energy. The active and passive anti-icing methods can realize surface deicing with extremely low energy consumption, high service life and low cost. How to reduce energy consumption and improve service life is a hot topic for researchers. Development of the efficient de-icing through decreasing the energy consumption is of great significance to realize energy saving and sustainable development in the related industries.

The main factors influencing the energy consumption of electric heating anti/de-icing are the heat dissipation to the icing surface, such as wings or blades, the heat dissipation in the ice, and the ice adhesion. However, the ice adhesion can be easily ignored in the electric heating anti/de-icing. As well known, the ice adhesion strength represents the interfacial bonding degree between ice and the materials, which determines the difficulty of de-icing^[18]. Using anti-icing materials can reduce the ice adhesion strength, and becomes one of the developing tendencies in advanced materials field^[19-21]. In recent decades, hydrophobic materials and coatings, by lowering the wettability of water, can achieve passive anti-icing, which are the hotspots for manufacturing the low-cost anti-icing materials. Golovin et al.^[22] prepared the polydimethylsiloxane (PDMS) gel by introducing silicone oil, and they found that the oil layer could reduce the ice adhesion to about 6.5 kPa. Wang et al.^[23] constructed an organogel through swelling cross-linked PDMS with liquid paraffin, and the ice adhesion was reduced to about 2.0 kPa.

Herein, we design an anti/de-icing surface based on the electric heating. The electrothermal structure is composed of PDMS insulation coating, conductive layer, electrothermal layer and porous insulation layer from the top to the bottom. The top

layer is the hydrophobic insulation layer, contributing to the low ice adhesion. The porous insulation layer can effectively prevent heat transfer to the substrate, greatly reducing energy loss. In this work, the influences of the conductive layer and electrothermal layer on heat transfer performance of the electrothermal material are investigated at different input powers. The energy utilization is evaluated according to the energy consumption of different structures. The main goal of this work is to find out the most energy-efficient electric heating anti/de-icing method.

1 Materials and Methods

1.1 Materials

Sodium chloride (NaCl) and anhydrous ethanol were purchased from Chengdu Kelon Chemical Co., Ltd. The conductive silver paste was purchased from Shenzhen Xinwei Electronic Materials Co., Ltd. The graphene conductive coating was purchased from Suzhou Carbonfeng Graphene Technology Co., Ltd. Graphene nano-sheet (diameter 1—3 μm) was purchased from Jiangsu Xianfeng Nano Material Technology Co., Ltd. PDMS prepolymer (Sylgard [®] 184, Dow Corning) and curing agent were provided by Shenzhen Xinhao Technology Co., Ltd., China.

1.2 Synthesis of electrothermal structure

1.2.1 Preparation of porous PDMS

The preparation diagram of porous PDMS is showed in Fig.1. PDMS oligomer was thoroughly mixed with the curing reagent at a weight ratio of 10:1. Then, excessive templates such as NaCl were added into the above sample and mixed about 10 min for well-distribution. After cured at 120 $^{\circ}\text{C}$ for 3 h in a vacuum drying oven, the PDMS filled with templates was prepared. Then, the PDMS was cut into 25 mm \times 25 mm \times 5 mm and ultrasonically cleaned with deionized water until the templates were removed.

1.2.2 Preparation of conductive layer and insulation

Preparation of a conductive layer (Fig.1) :

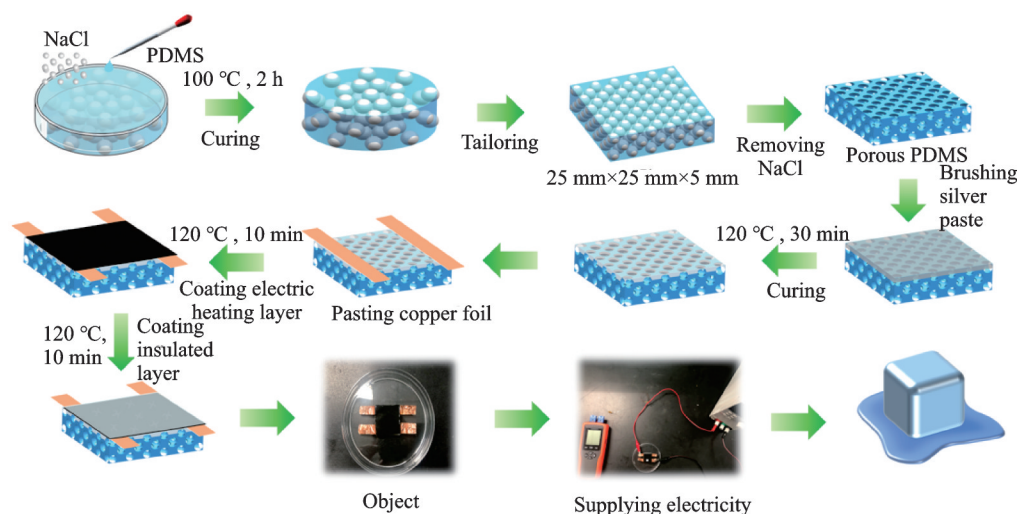


Fig.1 Schematic of preparation process of the electrothermal structure

Frist, 0.3 g conductive silver paste and 1.0 ml conductive silver paste diluent were fully diluted, and ultrasounded for 10 min. The above mixture with 0.1 g was evenly coated on the porous PDMS surface, and cured at 120 °C for 30 min. Then, two 55 mm × 6 mm copper foils were symmetrically pasted on the surface edge of the above surface. Subsequently, 1.0 g conductive silver paste, 2.0 ml graphene composite water-based conductive coating, 0.03 g graphene nano-sheet and 5.0 ml of anhydrous ethanol were well-mixed. Then, 0.5 ml the above solution was evenly coated on the surface of porous PDMS. The porous PDMS with the conductive layer was obtained after curing at 120 °C for 10 min. In addition, the porous PDMS under the conductive layer has the poor heat transfer effect, avoiding the downward transfer of heat and maximizing the use of energy.

Preparation of insulating layer: PDMS oligomer and curing agent was fully mixed at a mass ratio of 10:1. 0.25 ml of the above solution was coated on the surface of the conductive layer, spinning at 1 000 r/min for 30 s with glue homogenizer (KW4A, Sideka, China). The PDMS insulating layer coated on the conductive layer surface was obtained after cured at 100 °C for 10 min.

1.2.3 Characterization

The microstructure of superhydrophobic surface was characterized using Scanning electron microscopy (SEM, 7610F, Japan). Thermocouple

(WRNT-01, China) was used to test the temperature of the top layer and the bottom layer of the electrothermal structure at -20 °C and room environment. The thermal imager (FLIR, i7, USA) was used to record the temperature and temperature distribution of the top layer of the electrically heated structure. High-precision CNC DC regulated power supply (APS3005D, China) was used to input the different powers. The deicing performance of the superhydrophobic surface electric heating structure at low temperature was tested in the freezer (BD/BC-200FH, China) to ensure -20 °C.

1.2.4 Deicing test

The deicing test was conducted on the self-built experimental platform, which is composed of low-temperature ice chamber (-20 °C), loading platform, external DC power supply, thermocouple and a 90 g weight. The schematic diagram of the test platform is shown in Fig.2. The electric heating structure was fixed on the loading platform surface, and the two temperature sensors were arranged at the bottom of the porous PDMS and the surface of the insulating layer separately. An ice making mold (18 mm × 18 mm × 9 mm) was fixed on the porous PDMS insulation surface. The mold was injected deionized water to form icicles, being kept for 30 min at a low temperature to complete icing. During the test, the weight was connected to the ice mold locating 2.0 mm from the bottom edge through a thin wire. The temperature of the interface between

the ice and the insulating layer under different input powers, and the falling time of the weight were recorded.

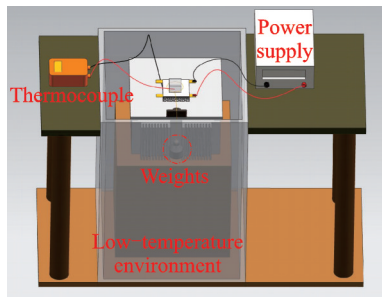


Fig.2 Schematic of the electric heating ice melting device

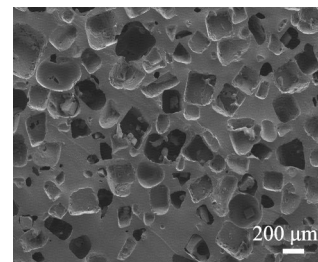
2 Results and Discussion

2.1 Analysis of the structure

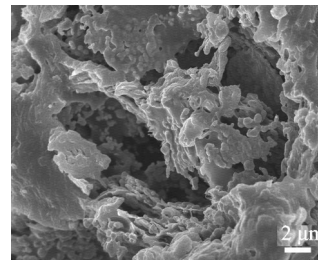
The composition and distribution of the electric heating structure were observed by SEM. As shown in Fig.3(a), the pore size of porous PDMS is about $400\ \mu\text{m}$, which is almost corresponding to the size of NaCl. In addition, the holes are interconnected channels, contributing to the great immersion of conductive silver paste solution and black conductive solution into the porous interior. Fig.3(b) shows that the conductive silver paste almost covers the PDMS holes surface, which benefits the formation of the conductive path. Fig.3(c) shows the structure of the electrothermal layer. It can be observed that a large amount of graphene is attached to the porous surface, contributing to the formation of the uniform temperature distribution on the surface. Fig.3(d) shows the top layer of PDMS insulation layer, which can effectively prevent circuit failures caused by ice melting. Fig.3(e) is the cross section of the electrothermal structure. It can be clearly distinguished that the electrothermal structure consists of the porous thermal insulation layer at the bottom and the conductive layer, electrothermal layer and insulating layer at the top layer. This structure is conducive to reducing the energy consumption in the deicing process and improving the energy utilization.

2.2 Analysis of electrothermal performance

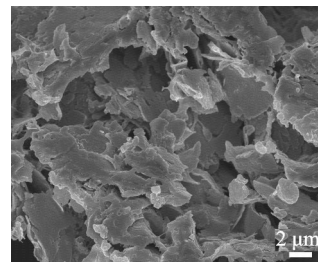
Fig.4 displays the maximum temperature and the temperature distribution influenced by the thickness of the silver paste layer at 1, 2 and 4 W. The



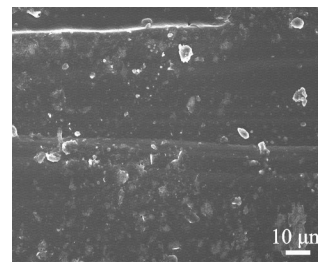
(a) Porous PDMS



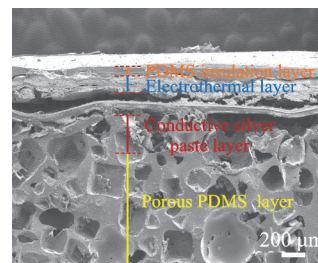
(b) Conductive silver paste



(c) Electrothermal layer



(d) PDMS insulation layer



(e) Cross-section of the electric heating structure

Fig.3 SEM images

result shows that the temperature is increased with the enhanced applied power and the temperature distribution on the top layer with the conductive silver paste is more uniform than that without conductive silver paste. As shown in Fig.4(a), the temperature of the top layer can reach $23\ ^\circ\text{C}$, $42\ ^\circ\text{C}$ and $112\ ^\circ\text{C}$ when the porous PDMS is only covered by

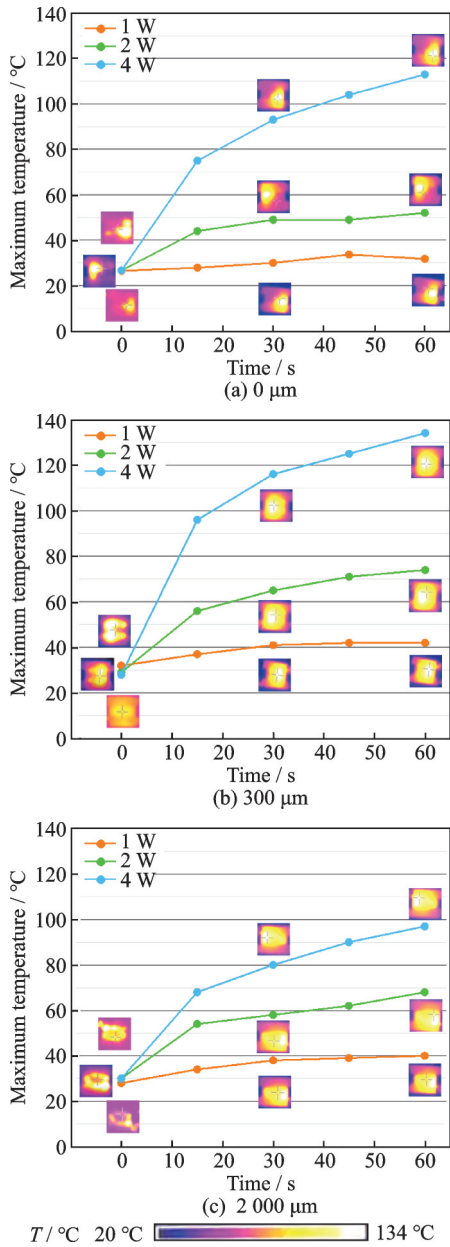


Fig.4 Temperature and temperature distribution with different thicknesses of the silver paste layers at different powers

the electrothermal layer. Moreover, the temperature distribution seems to be uneven without the conductive silver paste layer. Figs.4 (b, c) shows the temperature distribution when the thickness of conductive layer is 300 and 2 000 μm. By contrast, the temperature of the top layer with 300 μm conductive layer is higher than that with 2 000 mm conductive layer. As shown in Fig.4(b), the temperatures of the top layer are 40 °C, 78 °C and 134 °C when the input powers are 1, 2 and 4 W, which are obviously higher than that at 38 °C, 69 °C and 98 °C

in Fig.4(c). This is because the thin conductive layer is evenly distributed on the holes surface. Nevertheless, the thick conductive layer is easy to crack after curing, which inhibits the conductivity and results in the poor temperature rise.

Fig.5 provides the maximum temperature and the temperature distribution influenced by the thickness of the electric heating layer at 1, 2 and 4 W. In particular, 0.5, 1.5 and 3.0 ml represent the amount of conductive solution. With the increase of the amount of conductive solution, the thickness of the

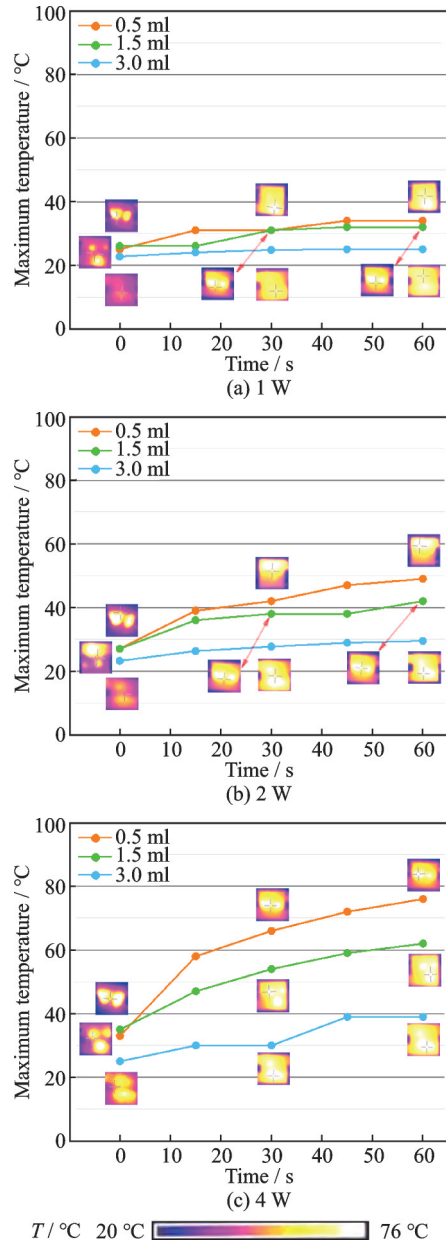


Fig.5 Temperature and temperature distribution when the amounts of conductive solution are 0.5, 1.5 and 3.0 ml

electro thermal layer increases. As shown in Fig.5(a), the maximum temperatures corresponding to 0.5, 1.5 and 3.0 ml conductive liquid are 34, 32 and 25 °C, respectively, at 1 W. Enhancing the input power, the maximum temperatures are increased. At 2 and 4 W, the max temperatures are 49 °C, 42 °C, 29.5 °C (Fig.5(b)), and 76 °C, 62 °C, 39 °C (Fig.5(c)), respectively. It is obvious that the thicker the electric heating layer, the worse the temperature rise. This is because the electric heating layer is cured in layers. The loose connection between layers probably results in the weakening of the electrical conductivity.

Fig.6 shows the temperatures of the top insulation layer and the bottom layer, and the average power of the electrically heated structure at the constant voltage of 0.5, 1, 2 and 3 V. It is found that the applied powers are 0.014, 0.057, 0.23, and 0.616 W/cm² at the constant voltage of 0.5, 1, 2, and 3 V, respectively. With the increasing voltage, the powers do not increase linearly because of the unstable current. The temperatures of the top layer are 28, 40, 76, and 170 °C when the input voltage are 0.5, 1, 2, and 3 V, respectively. And the corresponding temperatures of the bottom layer are 26, 27, 35, and 46 °C. The result indicates that the temperature difference between the top layers and the bottom surfaces are more and more obvious with the enhancing voltage, indicating that more and more heat is transferred to the top layer and used for deicing.

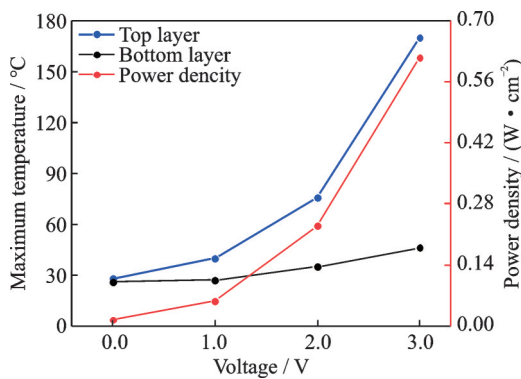


Fig.6 Maximum temperatures of the top layer and the bottom layer, and the average power of the electrically heated structure at constant voltages of 0.5, 1, 2 and 3 V

In order to analyze the energy utilization of the electrical heated structures, the energy-utilization ratio is calculated referred to the heat in thermodynamics and Joule's law^[24]. The total input energy and the energy absorbed by each layer are calculated according to the Eqs.(1,2). The energy-utilization ratios are calculated according to Eq.(3).

$$Q_1 = Pt \tag{1}$$

$$Q_2 = CM\Delta T \tag{2}$$

$$\eta = \left(1 - \sum Q_2 / Q_1\right) \times 100\% \tag{3}$$

where P is the input power; t the energizing time; C the specific heat capacity of the substance, where the specific heat capacity of PDMS is 1 100 J/(kg · K) and the specific heat capacity of graphene is 450 J/(kg · K)^[25-26]; M the mass and ΔT the temperature difference. The mass of PDMS insulation layer, electric heating layer of electrothermal layer and conductive silver paste layer and porous PDMS layer are 0.2, 0.8 and 1.65 g, respectively, in the electric heating structure. The temperature difference and the input power are referred to Fig.6.

The energy-utilization ratios are shown in Table 1. It is obvious that the enhancing input power increases the energy-utilization ratio. When the input power is 5.25 J, the energy-utilization ratio is 32.29%. Increasing the input power to 231.00 J, the energy-utilization ratio is 47.09%, which is almost increased by 31.43%. It is believed that the high input power enhances the temperature rise, and the ice attached to the surface can quickly melt and fall off. In this case, the energy lost in the heat transfer can be reduced, and therefore improve the energy-utilization ratio.

2.3 Analysis of deicing performance

In order to evaluate the energy utilization of the above electrothermal structure, the deicing experiment was carried out at -20 °C in the freezer. A 90 g weight was hung at the icicles, and the corresponding ice adhesion strength is 2.72 kPa. Fig.7 provides the ice column shedding time, and the temperatures of the top layer and the bottom surface at 1, 2, 4, 7 and 18 W. As shown in Fig.7(a), a larger power can promote the heat transfer to ice and

Table 1 Heat and energy utilization ratio of the electric heating structure of each layer

Voltage/V	Total energy/J	PDMS insulation layer/J	Electrothermal	Porous PDMS	Energy utilization
			layer and the conductive silver paste/J		
0.5	5.25	0.66	1.08	1.86	32.29
1	21.38	3.30	5.4	3.65	42.32
2	86.25	11.22	18.00	18.15	45.66
3	231.00	31.90	52.20	38.15	47.09

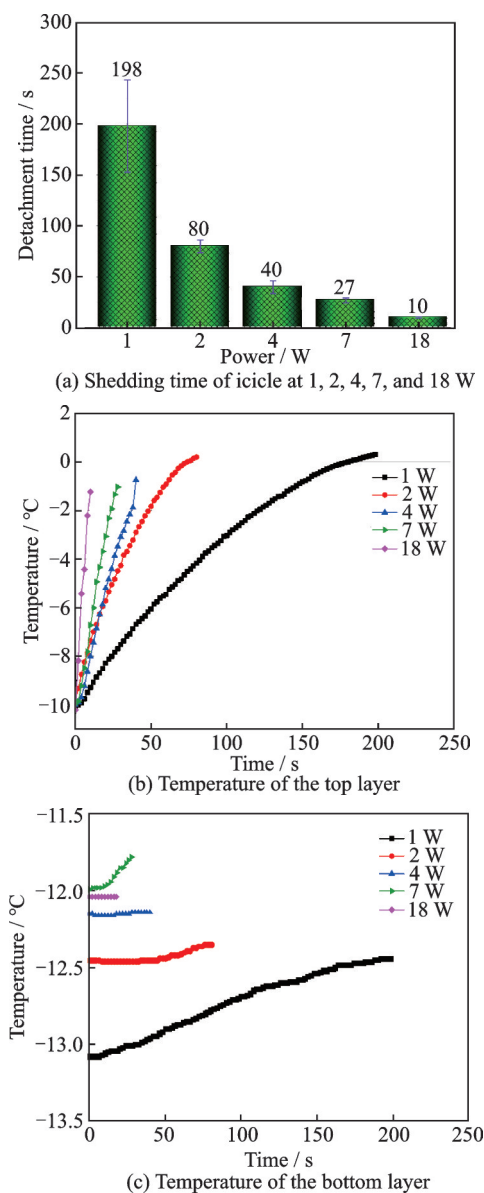


Fig.7 Shedding time referred to the time when the icicle falls off

shorter the shedding time. The shedding time is about 198 s when the input power is 1 W. Enhancing the power to 2 W, the shedding time is shorted to 80 s. When the input power is 18 W, the shedding time is about 10 s. The result indicates that a larger input power can increase the temperature rise rate of the top layer, making the icicle temperature

reach the melting point quickly. Figs.7(b, c) display the temperatures of the top layer and the bottom layer of the electrothermal structural material. It is found that the temperature of the top layer is quickly enhanced from $-10\text{ }^{\circ}\text{C}$ to $0\text{ }^{\circ}\text{C}$ at 18 W. When the input power is 1 W, the temperature rising rate is extremely slow. In this case, the rapid heating can reduce the energy loss during heating transfer. As shown in Fig.7(c), the bottom layer of the insulation layer heats up very slowly. When the power is 1 W, the temperature rise is about $0.5\text{ }^{\circ}\text{C}$, and the temperature change is less than $0.5\text{ }^{\circ}\text{C}$ at 2, 4, 7 and 18 W. It indicates that the porous PDMS can effectively inhibit the heat transfer at low temperatures, enhancing the energy utilization.

3 Conclusions

This paper innovatively designs an anti/detraining structure based on the electric heating. This structure is composed of PDMS insulation coating, conductive layer, electrothermal layer and porous insulation layer from the top to the bottom. The heat transfer is investigated by controlling the conductive layer and electrothermal layer at different input powers. The energy utilization is evaluated according to the energy consumption of different structure. Some conclusions are drawn as follows.

(1) The maximum temperature and the temperature distribution are influenced by the thickness of the silver paste layer. The thinner the silver paste layer, the better the temperature rise. The temperatures of the top layer can reach to $134\text{ }^{\circ}\text{C}$ when the input power is 4 W and the silver paste layer is $300\text{ }\mu\text{m}$.

(2) Similarly, when the amount of conductive solution is 0.5 ml, the temperature rises quickly. The electric heating layer is cured in layers. The

loose connection between layers probably results in the weakening of the electrical conductivity.

(3) When the electricity is in turn on process, the maximum energy-utilization ratio can reach to 47.09%, which suggests that more energy is used in the electro-thermal deicing process.

References

- [1] MA L, ZHANG Z, GAO L, et al. An exploratory study on using slippery-liquid-infused-porous-surface (SLIPS) for wind turbine icing mitigation[J]. *Renewable Energy*, 2020, 162: 2344-2360.
- [2] POURBAGIAN M, HABASHI W G. Aero-thermal optimization of in-flight electro-thermal ice protection systems in transient de-icing mode[J]. *International Journal of Heat and Fluid Flow*, 2015, 54: 167-182.
- [3] GUO L, CAO G, JI H. Numerical study on ridge ice accretion and its effect under thermal ice protection [J]. *Transactions of Nanjing University of Aeronautics and Astronautics*, 2018, 35(5): 770-777.
- [4] WU T, ZHANG B, CHEN M, et al. Flexural properties of electrothermal deicing composite laminates: Experimental and numerical study[J]. *Thin-Walled Structures*, 2022, 170: 108527.
- [5] ZHU Y, WANG Z, LIU X, et al. Anti-icing/de-icing mechanism and application progress of bio-inspired surface for aircraft[J]. *Transactions of Nanjing University of Aeronautics and Astronautics*, 2022, 39(5): 541-560.
- [6] NIU W, CHEN G, XU H, et al. Highly transparent and self-healable solar thermal anti-/deicing surfaces: When ultrathin mxene multilayers marry a solid slippery self-cleaning coating[J]. *Advanced Materials*, 2022, 34(10): 2108232.
- [7] ZHANG R, LIN P, YANG W, et al. Simultaneous superior lubrication and high load bearing by the dynamic weak interaction of a lubricant with mechanically strong bilayer porous hydrogels[J]. *Polymer Chemistry*, 2017, 8(46): 7102-7107.
- [8] DAI X, WEI Q, WANG Y, et al. A novel strategy to enhance the desalination stability of FAS (fluoroalkylsilane)-modified ceramic membranes via constructing a porous SiO₂@PDMS (polydimethylsiloxane) protective layer on their top[J]. *Chemical Engineering Journal*, 2022, 435: 134757.
- [9] KENZHEBAYEVA A, BAKBOLAT B, SULTANOV F, et al. A mini-review on recent developments in anti-icing methods[J]. *Polymers*, 2021, 13(23): 4149.
- [10] HOU Y, CHOY K L. Durable and robust PVDF-HFP/SiO₂/CNTs nanocomposites for anti-icing application: Water repellency, icing delay, and ice adhesion[J]. *Progress in Organic Coatings*, 2022, 163: 106637.
- [11] YU B, SUN Z, LIU Y, et al. Improving anti-icing and de-icing performances via thermal-regulation with macroporous xerogel[J]. *ACS Applied Materials & Interfaces*, 2021, 13(31): 37609-37616.
- [12] ZHANG Z, ZHOU J, REN Y, et al. Passive deicing CFRP surfaces enabled by super-hydrophobic multi-scale micro-nano structures fabricated via femtosecond laser direct writing[J]. *Nanomaterials*, 2022, 12(16): 2782.
- [13] IBANEZ-IBANEZ P F, RUIZ-CABELLO F J M, CABRERIZO-VÍLCHEZ M A, et al. Ice adhesion of PDMS surfaces with balanced elastic and water-repellent properties[J]. *Journal of Colloid and Interface Science*, 2022, 608: 792-799.
- [14] HE Z, ZHOU Y, HE J, et al. Design and preparation of sandwich-like polydimethylsiloxane (PDMS) sponges with super-low ice adhesion[J]. *Soft Matter*, 2018, 14(23): 4846-4851.
- [15] HANN R, ENACHE A, NIELSEN M C, et al. Experimental heat loads for electrothermal anti-icing and de-icing on uavs[J]. *Aerospace*, 2021, 8(3): 83.
- [16] HE Z, XIE H, JAMIL M I, et al. Electro-/photo-thermal promoted anti-icing materials: A new strategy combined with passive anti-icing and active de-icing[J]. *Advanced Materials Interfaces*, 2022, 9(16): 2200275.
- [17] SAMAD A, VILLENEUVE E, BLACKBURN C, et al. An experimental investigation of the convective heat transfer on a small helicopter rotor with anti-icing and de-icing test setups[J]. *Aerospace*, 2021, 8(4): 96.
- [18] QI H, LEI X, GU J, et al. Low modulus of polydimethylsiloxane organogel coatings induced low ice adhesion[J]. *Progress in Organic Coatings*, 2023, 177: 107435.
- [19] LI T, ZHOU Y, HAKONSEN V, et al. Durable low ice adhesion foams modulated by submicrometer pores[J]. *Industrial & Engineering Chemistry Research*, 2019, 58(38): 17776-17783.
- [20] LI J, JIAO W, WANG Y, et al. Research progress on application of superhydrophobic materials in anti-icing and de-icing technology[J]. *Acta Materiae Compositae Sinica*, 2022, 39(1): 16.
- [21] XIE Z, WANG H, ZHU X, et al. Preparation and anti-icing/deicing performance of photothermal superhydrophobic surfaces[J]. *CIESC Journal*, 2021, 72

- (11): 5840-5848.
- [22] GOLOVIN K, TUTEJA A. A predictive framework for the design and fabrication of icephobic polymers[J]. Science Advances, 2017, 3(9): e1701617.
- [23] WANG Y, YAO X, CHEN J, et al. Organogel as durable anti-icing coatings[J]. Science China Materials, 2015, 58: 559-565.
- [24] CHEN X, WANG Y, GU L, et al. Effect of joule heat effect, electrical breakdown and strain on I — V curve of single GaN nanowires[J]. Journal of Dalian Jiaotong University, 2019, 40(3): 92-96.
- [25] CAO J, HONG F, ZHENG P. Numerical study on joule heating effect in PDMS microfluidic chip[J]. Journal of Engineering Thermophysics, 2009, 30(1): 124-128.
- [26] WEI L, LIU D, LIANG J. Fire retardancy and thermal conductivity properties of PP/GNPs nano-platelets composites[J]. Engineering Plastics Application, 2016, 44(10): 98-101.

Acknowledgement This work was funded by the National Natural Science Foundations of China (No.52105214), Sichuan Science and Technology Program (No.2022NSF-SC1928), and the Key Laboratory of Icing and Anti/De-icing of CARDC (Nos.IADL 20210403, IADL20210103).

Authors Mr. GU Jianzhen received his B.S. degree in Me-

chanical Design and Manufacturing and Automation from Southwest University of Science and Technology (SWUST) in 2021. From 2021 to present, he has been a graduate student in the School of Manufacturing Science and Engineering at SWUST. His main research interests are electric heating anti/de-icing.

Prof. **QI Huimin** received her Ph. D. degree of Materials from Lanzhou Institute of Chemical Physics, Chinese Academy of Sciences in 2018. Now she is a professor at College of Mechanical and Electrical Engineering in Southwest University of Science and Technology. Her research interests include self-lubricated composites, surface engineering.

Author contributions Mr. **GU Jianzhen** contributed to data analysis on the anti/de-icing performance, and wrote the manuscript. Prof. **QI Huimin** designed the study, and conducted the analysis. Prof. **YU Jiabin** contributed to the discussion and background of the study. Prof. **ZHANG Yafeng** contributed to the discussion and background of the study. Dr. **GU Xingshi** interpreted the results and contributed to data analysis on the anti/de-icing performance. All authors commented on the manuscript draft and approved the submission.

Competing interests The authors declare no competing interests.

(Production Editor:ZHANG Bei)

新型电热结构防除冰性能研究

谷建臻¹, 齐慧敏¹, 余家欣¹, 张亚锋¹, 顾兴士²

(1.西南科技大学制造过程测试技术教育部重点实验室, 绵阳621010, 中国; 2.中国空气动力研究与发展中心结冰与防除冰重点实验室, 绵阳621000, 中国)

摘要:创新性地开发机翼电热防/除冰系统仍然是航空航天领域面临的巨大挑战,提高电热防/除冰系统的能量利用率受到了防除冰领域专家的广泛关注。本文创新性地设计了一种多孔电热防除冰结构,多孔基体通过模板法制备得到。电热结构从上至下由绝缘涂层、导电层、电热层和隔热层组成。研究了导电银浆层厚度及导电液含量在不同功率下绝缘层和隔热层的温度变化。结果表明,室温条件下,当输入功率为4 W、银浆层厚度为300 μm时,绝缘层的温度最高可达134℃。在-20℃的冰脱落实验中,发现当输入功率为18 W时,顶层温度可快速达到0℃,而底层温度维持在-12.5℃左右,能量损失较少。本文可为电热防除冰材料体系的设计提供理论指导。

关键词:防冰;电热结构;聚二甲基硅氧烷;传热;能量利用